

Novel Role of Superfluidity in Low-Energy Nuclear Reactions

Piotr Magierski^{1,2}, Kazuyuki Sekizawa¹, Gabriel Wlazłowski^{1,2}

¹*Faculty of Physics, Warsaw University of Technology,
Ulica Koszykowa 75, 00-662 Warsaw, Poland and*

²*Department of Physics, University of Washington, Seattle, Washington 98195-1560, USA**

We demonstrate, within symmetry unrestricted time dependent density functional theory, the existence of new effects in low-energy nuclear reactions which originate from superfluidity. The dynamics of the pairing field induces solitonic excitations in the colliding nuclear systems, leading to qualitative changes in the reaction dynamics. The solitonic excitation prevents collective energy dissipation and effectively suppresses capture cross section. We demonstrate how the variations of the total kinetic energy of the fragments can be traced back to the energy stored in the superfluid junction of colliding nuclei. Both contact time and scattering angle in non-central collisions are significantly affected. The modification of the capture cross section and possibilities for its experimental detection are discussed.

PACS numbers: 25.70.-z, 25.70.Jj, 03.75.Lm, 74.40.Gh

Introduction.— Dynamics of the pairing field during the nuclear reactions has rarely been investigated to date, although it is well-known that the static pairing field is crucial for the description of the atomic nuclei, both in the ground state as well as in excited states, involving large-amplitude collective motions (see, *e.g.*, [1–5] and references therein). The reason is twofold: first, it is believed that the pairing field dynamics will produce only small corrections to the commonly accepted picture of low-energy nuclear reactions; second, the proper treatment of the pairing field dynamics requires to use more advanced approach resulting in rapid increase of computational complexity.

The pairing field in nuclear systems is small in a sense that the ratio of its magnitude to the Fermi energy does not exceed 5%. It implies that BCS treatment is regarded as a justified approximation and the size of the Cooper pair is of the same order as the size of a heavy nucleus. Although the pairing field is small as compared to, *e.g.*, the unitary Fermi gas [6], it is important for the proper description of the nuclear systems: it makes a nucleus more susceptible towards deformations, and it allows for large-amplitude collective motion which otherwise would be strongly damped. Therefore the description of large-amplitude collective motion, like nuclear fission, requires to take into account superfluidity as one of crucial ingredients [7–9]. However, the static treatment of the pairing field during the time evolution misses part of the degrees of freedom related to the dynamics of Cooper pairs. Recently, it has been pointed out that these excitation modes of the pairing field affect significantly the induced fission process leading to much longer fission timescales than predicted by other simplified approaches [10].

The pairing field $\Delta(\mathbf{r})$ can be regarded as an order parameter that specifies whether the nucleus is superfluid or not. The superfluid order parameter belongs to U(1) universality class and it can be decomposed as $\Delta(\mathbf{r}) = |\Delta(\mathbf{r})|e^{i\varphi(\mathbf{r})}$. The phase φ is closely related to the

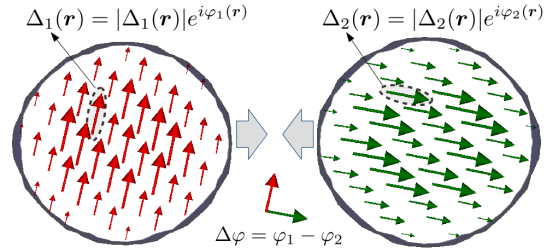


FIG. 1: (Color online) Schematic picture of the situation we examine in the present Letter: a collision of two superfluid nuclei with different phases of the pairing fields. Each disc represents a cross section of a nucleus. The arrows inside the nucleus indicate the pairing field $\Delta_i(\mathbf{r})$ where length of the arrow indicates its absolute value $|\Delta_i(\mathbf{r})|$, while direction indicates its phase $\varphi_i(\mathbf{r})$ ($i = 1, 2$). In the ground state, the phase is uniform across each nucleus $\varphi_i(\mathbf{r}) = \varphi_i$ and the phase difference $\Delta\varphi$ ($\equiv \varphi_1 - \varphi_2$) is well defined. We will show how the phase difference affects the reaction dynamics.

phase of the Cooper-pair wave function. In the ground state the phase is uniform across the nucleus, and it can be absorbed by the normalization factor of the wave function. Then the only relevant quantity is its absolute value $|\Delta(\mathbf{r})|$ which is on the order of 1 MeV. The situation is different when two superfluid nuclei are considered. Then the relative phase $\Delta\varphi$ between two pairing fields is well defined (see Fig. 1) and cannot be removed from the total wave function describing both nuclei. This difference will trigger various excitation modes of the pairing field as well as the particle flow between colliding nuclei. Although the phases of the pairing fields are not controlled in nuclear experiments, they will affect the reaction outcomes in an averaged way. The consequences of this effect turn out to be significant and are discussed in this Letter.

Collision of two superfluid nuclei.— Let us first focus on the energy scale of the possible effect which may appear during a collision of two superfluid nuclei at a fixed

pairing phase difference $\Delta\varphi$. One would naively expect that it is governed by the pairing energy which is proportional (for protons or neutrons) to $\frac{1}{2}g(\varepsilon_F)|\Delta|^2$, where $g(\varepsilon_F)$ represents the density of states per one spin projection at the Fermi level, and Δ is the pairing gap. Such quantity for nuclei is on the order of MeV, and thus one may infer that the possible effects would be too weak to be observed in nuclear reactions. However, this is not the case since during the collision a junction between two superfluids is created, where the phase varies rapidly. Consequently, the energy stored in the junction depends both on the phase difference and the size of the junction. One may estimate the energy of the junction from the Ginzburg-Landau (G-L) approach:

$$E_j = \frac{S}{L} \frac{\hbar^2}{2m} n_s \sin^2 \frac{\Delta\varphi}{2}, \quad (1)$$

where S is the area of the junction, L is the length scale over which the phase varies, and n_s is the superfluid density (for derivation, see [11]). Note that neither the pairing energy, nor the pairing gap enters this formula. For a collision of two heavy nuclei at energies close to the Coulomb barrier, one may assume the area of the junction S corresponds to the neck, which is on the order of πR^2 with $R \approx 6$ fm, and taking $L \approx R$ and n_s as a half of nuclear density, one finds that the energy of the junction varies by several tens of MeV. Such a drastic energy change may significantly alter the dynamics of the collision. Clearly in order to determine those quantities in Eq. (1) (S, L, n_s) one needs to perform microscopic simulations, since they are in general dependent on the actual reaction dynamics. It is to be reminded that the energy scale involved here is of the same order as the so-called extra-push energy introduced by Swiatecki to explain the experimental fusion cross sections for collisions of medium and heavy nuclei at energies above the Coulomb barrier [16–18]. The situation during the collision of two nuclei possessing different phases of the pairing fields resembles also the Josephson junction encountered in solids and ultracold atomic gases. However in the case of nuclear reactions the important observables are different. Apart from possible Josephson current [19–23], which we will address later, the natural question concerns the impact of the pairing field dynamics on the fusion cross section and the total kinetic energy (TKE) of the fragments.

In experiments with ultracold atomic gases, where two clouds of atomic BECs of different phases are forced to merge, the dark soliton is created which is unstable and decays producing quantum vortices [24–26]. In collisions of superfluid nuclei possessing different phases, one should observe an analogue of the solitonic excitation. The questions of crucial importance are related to the size of the soliton and its lifetime. There are several ingredients that may influence these two factors, as we expect that the solitonic solution will eventually dissipate,

and the way and the characteristic time of the dissipation depend on details related to, *e.g.*, the strength of the Josephson current and coupling to Bogoliubov phonons.

TDSLDA for nuclear reactions.— Presently, the most accurate microscopic approaches to the dynamics of superfluid systems are based on the density functional theory. While the underlying equations are very similar to the mean-field equations, the method is in principle exact. Here we utilize the formulation known as time-dependent superfluid local density approximation (TDSLDA)—the approach proved to be very accurate for describing dynamics of strongly correlated fermionic systems, like ultracold atomic gases [26–32] and nuclear systems [10, 33–35]. We solve the TDSLDA equations numerically on a 3D spatial lattice (without any symmetry restrictions) with periodic boundary conditions. We use a box of size 80 fm \times 25 fm \times 25 fm for head-on collisions and 80 fm \times 60 fm \times 25 fm for non-central collisions. The lattice spacing is set to 1.25 fm. For the energy density functional, we use FaNDF⁰ functional [36, 37] without the spin-orbit term.

Although it is well known that the spin-orbit interaction is crucial for the proper description of nuclear static properties, for the purpose of this Letter it is of secondary importance. In this Letter, we investigate possible impact of the phase difference on the reaction dynamics and address the following questions: what observables are affected by the phase difference and for each affected quantity what is the predicted size of the effect? In order to answer these questions one needs to set correctly the scales of the problem, which in the context of pairing dynamics are determined by the average magnitude of the pairing gap and the coherence length to the system size ratio. None of the meaningful scales in our problem is affected by the spin-orbit interaction. However, in order to provide results that can be compared directly with experimental data, one needs to perform calculations with a full nuclear density functional. We defer these extremely numerically expensive studies to future works. This simplification allows us to construct a highly efficient solver of the TDSLDA equations (for details, see supplemental material of [12]). Nevertheless, problem is still numerically demanding and requires usage of supercomputers.

Finally, we emphasize that effects studied in this Letter are clearly beyond microscopic approaches based on TDHF+BCS approximation [38–42].

One may rise a question regarding the adequacy of the description of the finite system using the theoretical framework admitting the broken particle-number symmetry. It gives rise to the Nambu-Goldstone (NG) modes related to the rotation of the phase of the pairing field [43, 44]. The phase can be traced back to the phase of the Cooper-pair wave function, which can be defined as the eigenfunction corresponding to the dominant eigenvalue of the two-body density matrix, and thus, is independent of a particular approximation in the treatment of

the pairing correlations. The particle-number projected (symmetry restored) wave function would imply averaging over the phase. The natural question is whether this averaging needs to be performed before the collision. The answer to this question is related to the timescale of the associated NG mode, which is governed by the nuclear chemical potentials. Since phases of both projectile and target nuclei rotate during the time evolution, what matters is the difference of the periods of the pairing phase rotations. If it is long enough as compared to the timescale of the collision, the use of the framework with broken particle-number symmetry is validated [45]. In the case of nuclear collision it is determined by the difference of separation energies of the projectile and target nuclei $\Delta S = |S_1 - S_2|$. Thus, the description will be valid if one limits to the collision of nuclei whose difference between the separation energies does not exceed 1 MeV that leads $T = \frac{2\pi\hbar}{\Delta S} > 1200 \text{ fm}/c$ which is longer than the collision time. The most clean case corresponds to the symmetric collision where the phase difference does not depend on time.

Kinetic energy and Josephson current.— As a first example, we consider symmetric collisions of two heavy nuclei. In such a case the two nuclei do not fuse and re-separate shortly after collision. In terms of number of protons and neutrons our colliding objects correspond to ^{240}Pu , but since the spin-orbit term is neglected the nucleus does not exhibit a prolate deformation. In Fig. 2, we show pairing fields and densities of the colliding nuclei at various times in two extreme cases: $\Delta\varphi = 0$ and $\Delta\varphi = \pi$. It is clearly visible that in the $\Delta\varphi = \pi$ case the narrow solitonic structure is created, which stays there until the composite system splits. This produces a significant impact on resulting TKE of the fragments. In Fig. 3 (a), we show the TKE as a function of the relative phase for various collision energies. The TKE clearly shows the $\sin^2 \frac{\Delta\varphi}{2}$ pattern (gray solid curves), which exactly recovers the dependence of the energy of the junction given by the G-L approach, Eq. (1). The dominating contribution comes from the neutron pairing field. The contribution from the proton pairing field is less than 30% of the neutron effect, due to Coulomb repulsion [11]. These results indicate that the phase difference hinders the energy transfer from the relative motion to internal degrees of freedom.

The situation becomes qualitatively different when the energy is further increased. Namely, at energies about 30% above the barrier, the departure from this simple pattern is observed. It corresponds to the energies at which the third light fragment is observed [11]. Taking into account that the barrier height in this case is about $V_{\text{Bass}} \approx 900 \text{ MeV}$, it corresponds to the case when the available energy for colliding nuclei is on the order of 270 MeV. For such energies one would expect that energies are too high to follow exactly the pattern based on the static G-L approach. The appearance of the third

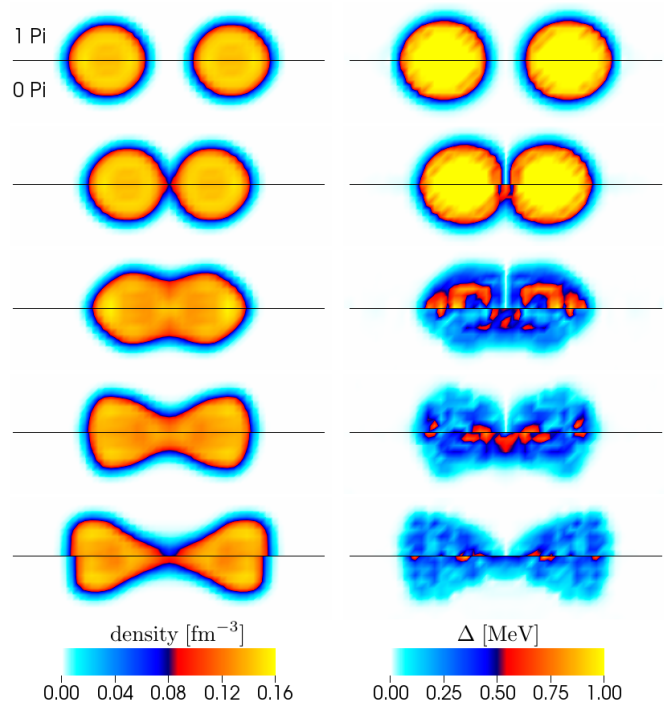


FIG. 2: (Color online) Snapshots from the collision of $^{240}\text{Pu} + ^{240}\text{Pu}$ for two extreme values of the relative phase differences ($\Delta\varphi = 0$ and π) at the energy $E \simeq 1.1V_{\text{Bass}}$, where V_{Bass} represents the phenomenological fusion barrier [14]. Left panels show the total density distribution, whereas the right panels show the neutron pairing field of two colliding nuclei. Top half of each panel corresponds to the phase difference $\Delta\varphi = \pi$, while bottom half corresponds to the case without phase difference $\Delta\varphi = 0$. Contact time is about 550–600 fm/c depending on the phase difference. For movies, see [11].

light fragment in the quasifission process is understood as a consequence of the density and charge excesses in the neck region [15]. However the solitonic excitation decreases effectively the density in the neck region. Consequently, for the energy range $1.3V_{\text{Bass}} < E < 1.5V_{\text{Bass}}$ the number of fragments depends on the phase difference and smaller phase differences favors the emission of the third fragment [11]. For $E > 1.5V_{\text{Bass}}$ splitting into three fragments is observed for all phase differences.

Let us investigate the Josephson current between colliding nuclei induced by the phase difference. Even though the reaction is symmetric, it can cause nucleon transfer from one nucleus to the other. Indeed, we observe that after re-separation the fragments are not symmetric. However, the amount of nucleon transfer does not exceed 1.5 for neutrons and 0.5 for protons during the collision (see, Fig. 3 (b) and [11] for more details). This weakness of Josephson current is consistent with earlier studies [19–23]. By the same amount the Josephson current affects the particle transfer in asymmetric reactions [11]. Note that this weak current is responsible for the stability of the solitonic structure, as the

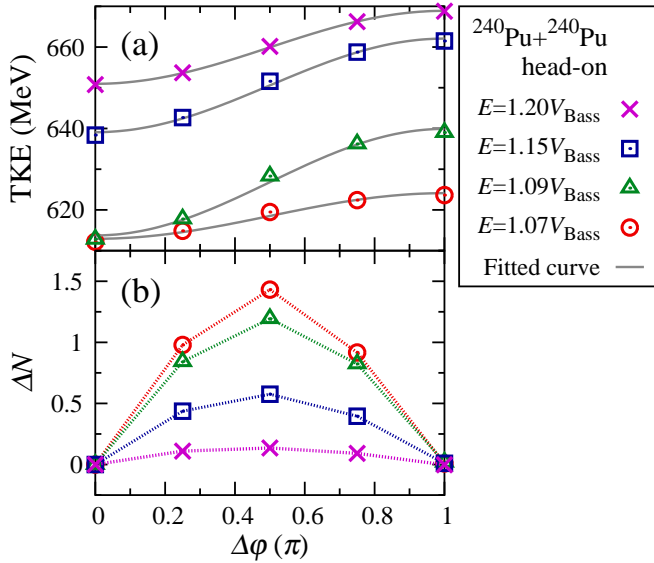


FIG. 3: (Color online) Results of the TDSFDA simulations for $^{240}\text{Pu}+^{240}\text{Pu}$ head-on collisions at various collision energies. (a): Total kinetic energy (TKE) of the outgoing fragments is shown. Line shows fit to the data by a formula $\alpha + \beta \sin^2 \frac{\Delta\phi}{2}$ with respect to parameters α and β . (b): The average number of transferred neutrons from the left nucleus to the right nucleus due to the Josephson current is shown. The horizontal axis is the relative pairing phase $\Delta\phi$.

Josephson current is the most efficient way for the phase exchange of the pairing fields.

Energy threshold for fusion.— Results for a heavy system indicate that the phase difference effectively works as a potential barrier, and consequently will affect the fusion cross section. In order to investigate this issue, we examine collisions of two medium mass nuclei that can fuse. Now, number of protons and neutrons for colliding objects correspond to ^{90}Zr . Note that when the spin-orbit term is dropped this is an open-shell nucleus for neutrons and thus neutrons are superfluid, whereas protons have a closed shell. In Fig. 4, we show the minimum energy required for the system to merge in head-on collisions and stay in contact for times longer than 12 000 fm/c (40 zs). The results clearly demonstrate that the effective barrier for fusion is increased by the dynamic excitations of the pairing field. The energy threshold as a function of the angle does not have $\sin^2 \frac{\Delta\phi}{2}$ dependence, since we consider now collisions varying both the phase difference and the energy.

The fusion hindrance phenomenon may likely be observed by studies of the fusion cross section for symmetric collisions at the vicinity of the barrier, in a similar way to experimental detection of the extra-push energy [46, 47]. As a good candidate we suggest symmetric reactions with different Zr isotopes. For these reactions the extra-push energy is negligible. ^{90}Zr is neutron magic and the pairing correlations are absent. Thus, in this case one ex-

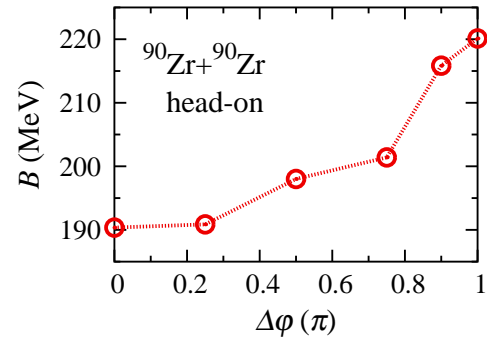


FIG. 4: (Color online) Results of the TDSFDA simulations for $^{90}\text{Zr}+^{90}\text{Zr}$ head-on collisions. Fusion threshold energy B is shown as a function of the relative pairing phase $\Delta\phi$. For this reaction the barrier height is $V_{\text{Bass}} \simeq 192$ MeV. The phase difference prevents fusion for energies up to 15% above the barrier.

pects no hindrance due to the pairing effects. As the neutron number increases neutrons become superfluid which results in an increase of the barrier height. Based on our results the barrier change is expected to be about $E_{\text{extra}} = \frac{1}{\pi} \int_0^\pi (B(\Delta\phi) - V_{\text{Bass}}) d(\Delta\phi) \approx 10$ MeV on average.

Another possibility is to investigate asymmetric reactions like $^{90-96}\text{Zr}+^{124}\text{Sn}$. Despite the fact that the extra-push model predicts that the hindrance of the fusion cross section becomes weaker with increasing the neutron excess, the experimental data suggest the opposite trend [46]. This agrees with the results presented here, as the effect is better pronounced as the system departs from the neutron magic ^{90}Zr . The chemical potentials for colliding nuclei are fairly similar admitting the description within broken particle-number symmetry. For these nuclei the difference in neutron separation energies are about $|\Delta S_n| \approx 0.6, 0.3, 0.1$ MeV for $^{96,94,92}\text{Zr}$, respectively. We have performed exploratory simulations for asymmetric reactions, and we have found that, similarly to the symmetric case, the phase difference can hinder the fusion for energies around the barrier, however no clear solitonic structure was observed [11].

Finally, we have also performed simulations of non-central collisions. If we are in the energy window where the phase difference can hinder the fusion, we find that it affects the contact time. Since the composite system rotates the phase difference causes the reparation at different times and scattering angle is affected (see, [11] for movies demonstrating this effect).

Summary.— We have investigated collisions of medium and heavy nuclei at energies around the Coulomb barrier taking into account the pairing field dynamics with TDDFT extended to superfluid systems. We have found that during collision a stable soliton-like structure appears when two superfluid nuclei collide with the phase difference of the pairing fields close to $\Delta\phi = \pi$. The soli-

tonic excitation suppresses the neck formation and hinders energy dissipation as well as fusion reaction, leading to significant changes in reaction dynamics. It implies that the pairing field dynamics effectively increases the barrier height for fusion resembling “thud wall” in the extra-push model, although at much smaller energies. The Josephson current between two fragments turns out to be small, does not exceed 2 particles. The effects on the kinetic energy of the fragments and fusion cross section may likely be observed experimentally.

We are in particular grateful to George Bertsch and Aurel Bulgac for discussions and critical remarks. We would like also to thank Nicholas Keeley, Michal Kowal, Eryk Piasecki, Krzysztof Rusek, Janusz Skalski for helpful discussions. We thank Witold Rudnicki, Franciszek Rakowski, Maciej Marchwiany and Kajetan Dutka from the Interdisciplinary Centre for Mathematical and Computational Modelling (ICM) of Warsaw University for useful discussions concerning the code optimization. This work was supported by the Polish National Science Center (NCN) under Contracts No. UMO-2013/08/A/ST3/00708. The code used for generation of initial states was developed under grant of Polish NCN under Contracts No. UMO-2014/13/D/ST3/01940. Calculations have been performed at HA-PACS (PACS-VIII) system—resources provided by Interdisciplinary Computational Science Program in Center for Computational Sciences, University of Tsukuba. The contribution of each one of the authors has been significant and the order of the names is alphabetical.

* Electronic address: magiersk@if.pw.edu.pl, sekizawa@if.pw.edu.pl, gabrielw@if.pw.edu.pl

- [1] P. Ring and P. Schuck, *The Nuclear Many-Body Problem* (Springer-Verlag, Berlin, 2000).
- [2] Y.R. Shimizu, J.D. Garrett, R.A. Broglia, M. Gallardo, and E. Vigezzi, Pairing fluctuations in rapidly rotating nuclei, *Rev. Mod. Phys.* **61**, 131 (1989).
- [3] M. Bender, P.-H. Heenen, and P.-G. Reinhard, Self-consistent mean-field models for nuclear structure, *Rev. Mod. Phys.* **75**, 121 (2003).
- [4] D.J. Dean and M. Hjorth-Jensen, Pairing in nuclear systems: from neutron stars to finite nuclei, *Rev. Mod. Phys.* **75**, 607 (2003).
- [5] Y. Hashimoto, Time-dependent Hartree-Fock-Bogoliubov calculations using a Lagrange mesh with the Gogny interaction, *Phys. Rev. C* **88**, 034307 (2013).
- [6] The BCS-BEC Crossover and the Unitary Fermi Gas, *Lecture Notes in Physics* **836**, ed. W. Zwerger, (Springer-Heidelberg 2012).
- [7] G.F. Bertsch, The nuclear density of states in the space of nuclear shapes, *Phys. Lett.* **B95**, 157 (1980).
- [8] F. Barranco, G.F. Bertsch, R.A. Broglia, and E. Vigezzi, Large-amplitude motion in superfluid Fermi droplets, *Nucl. Phys.* **A512**, 253 (1990).
- [9] G.F. Bertsch, Large amplitude collective motion, *Nucl. Phys.* **A574**, 169c (1994).
- [10] A. Bulgac, P. Magierski, K.J. Roche, and I. Stetcu, Induced Fission of ^{240}Pu within a Real-Time Microscopic Framework, *Phys. Rev. Lett.* **116**, 122504 (2016).
- [11] See Supplemental Material at {URL will be provided by the publisher} for discussion of technical aspects including generation of initial configurations, derivation of energy of the junction, supplemental results, and list of movies, which includes Refs. [12–15].
- [12] G. Wlazowski, K. Sekizawa, P. Magierski, A. Bulgac, M.M. Forbes, Vortex pinning and dynamics in the neutron star crust, *Phys. Rev. Lett.* (in press); arXiv:1606.04847.
- [13] S. Jin, A. Bulgac, K. Roche, and G. Wlazowski, Coordinate-Space Solver for Superfluid Many-Fermion Systems with Shifted Conjugate Orthogonal Conjugate Gradient Method, (2016), arXiv:1608.03711 [nucl-th].
- [14] R. Bass, Fusion of heavy nuclei in a classical model, *Nucl. Phys.* **A231**, 45 (1974).
- [15] C. Golabek and C. Simenel, Collision dynamics of two ^{238}U atomic nuclei, *Phys. Rev. Lett.* **103**, 042701 (2009).
- [16] W.J. Swiatecki, The dynamics of the fusion of two nuclei, *Nucl. Phys.* **A376**, 275 (1982).
- [17] S. Bjornholm and W.J. Swiatecki, Dynamical aspects of nucleus-nucleus collisions, *Nucl. Phys.* **A391**, 471 (1982).
- [18] R. Donangelo, L.F. Canto, Studies of nucleus-nucleus collisions with a schematic liquid-drop model and one-body dissipation, *Nucl. Phys.* **A451**, 349 (1986).
- [19] K. Dietrich, On a nuclear Josephson effect in heavy ion scattering, *Phys. Lett.* **B32**, 428 (1970).
- [20] K. Dietrich, Semiclassical Theory of a Nuclear Josephson Effect in Reactions between Heavy Ions, *Ann. Phys.* (N.Y.) **66**, 480, (1970).
- [21] K. Dietrich, K. Hara, and F. Weller, Multiple pair transfer in reactions between heavy nuclei, *Phys. Lett. B* **35**, 201 (1971).
- [22] J. H., Sorensen and A. Winther, Multipair transfer in collisions between heavy nuclei, *Phys. Rev. C* **47**, 1691 (1993).
- [23] Y. Hashimoto and G. Scamps, Gauge angle dependence in TDHFB calculations of $^{20}\text{O}+^{20}\text{O}$ head-on collisions with the Gogny interaction, *Phys. Rev. C* **94**, 014610 (2016).
- [24] M.J.H. Ku, W. Ji, B. Mukherjee, E. Guardado-Sanchez, L. W. Cheuk, T. Yefsah, and M. W. Zwierlein, Motion of a Solitonic Vortex in the BEC-BCS Crossover, *Phys. Rev. Lett.* **113**, 065301 (2014).
- [25] M.J.H. Ku, B. Mukherjee, T. Yefsah, and M.W. Zwierlein, Cascade of Solitonic Excitations in a Superfluid Fermi gas: From Planar Solitons to Vortex Rings and Lines, *Phys. Rev. Lett.* **116**, 045304 (2016).
- [26] G. Wlazowski, A. Bulgac, M.M. Forbes, and K.J. Roche, Life Cycle of Superfluid Vortices and quantum turbulence in the Unitary Fermi Gas, *Phys. Rev. A* **91**, 031602(R) (2015).
- [27] A. Bulgac and S. Yoon, Large Amplitude Dynamics of the Pairing Correlations in a Unitary Fermi Gas, *Phys. Rev. Lett.* **102**, 085302 (2009).
- [28] A. Bulgac, Y.-L. Luo, P. Magierski, K.J. Roche, and Y. Yu, Real-Time Dynamics of Quantized Vortices in a Unitary Fermi Superfluid, *Science* **332**, 1288 (2011).
- [29] A. Bulgac, P. Magierski, and M.M. Forbes, The Unitary Fermi Gas: From Monte Carlo to Density Functionals, in *BCS-BEC Crossover and the Unitary Fermi Gas*, edited by W. Zwerger, *Lecture Notes in Physics*, Vol. **836**, pp

- 305-373 (Springer, Heidelberg, 2012).
- [30] A. Bulgac, Y.-L. Luo, and K.J. Roche, Quantum Shock Waves and Domain Walls in Real-Time Dynamics of a Superfluid Unitary Femi Gas, *Phys. Rev. Lett.* **108**, 150401 (2012).
 - [31] A. Bulgac, Time-Dependent Density Functional Theory and Real-Time Dynamics of Fermi Superfluids, *Ann. Rev. Nucl. Part. Sci.* **63**, 97 (2013).
 - [32] A. Bulgac, M.M. Forbes, M.M. Kelley, K.J. Roche, and G. Wlazłowski, Quantized Superfluid Vortex Rings in the Unitary Fermi Gas, *Phys. Rev. Lett.* **112**, 025301 (2014).
 - [33] I. Stetcu, A. Bulgac, P. Magierski, and K.J. Roche, Isovector Giant Dipole Resonance from 3D Time-Dependent Density Functional Theory for Superfluid Nuclei, *Phys. Rev. C* **84**, 051309(R) (2011).
 - [34] I. Stetcu, C.A. Bertulani, A. Bulgac, P. Magierski, and K.J. Roche, Relativistic Coulomb Excitation within Time-Dependent Superfluid Local Density Approximation, *Phys. Rev. Lett.* **114**, 012701 (2015).
 - [35] P. Magierski, Nuclear Reactions and Superfluid Time Dependent Density Functional Theory, invited paper honoring Prof. Joachim Maruhn's retirement to be published as a chapter in "Progress of time-dependent nuclear reaction theory" (ed. Yoritaka Iwata) in the ebook series: "Frontiers in nuclear and particle physics" (Bentham Science Publishers); arXiv:1606.02225.
 - [36] S.A. Fayans, Towards a universal nuclear density functional, *JETP Letters* **68**, 169 (1998).
 - [37] S.A. Fayans, S.V. Tolokonnikov, E.L. Trykov, and D. Zawischa, Nuclear isotope shifts within the local energy-density functional approach, *Nucl. Phys.* **A676**, 49 (2000).
 - [38] S. Ebata, T. Nakatsukasa, T. Inakura, K. Yoshida, Y. Hashimoto, and K. Yabana, Canonical-basis time-dependent Hartree-Fock-Bogoliubov theory and linear-response calculations, *Phys. Rev. C* **82**, 034306 (2010).
 - [39] G. Scamps, D. Lacroix, G.F. Bertsch, and K. Washiyama, Pairing dynamics in particle transport, *Phys. Rev. C* **85**, 034328 (2012).
 - [40] G. Scamps and D. Lacroix, Effect of pairing on one- and two-nucleon transfer below the Coulomb barrier: A time-dependent microscopic description, *Phys. Rev. C* **87**, 014605 (2013).
 - [41] G. Scamps and D. Lacroix, Effect of pairing on transfer and fusion reactions, *EPJ Web of Conf.* **86**, 00042 (2015).
 - [42] S. Ebata and T. Nakatsukasa, Repulsive Aspects of Pairing Correlation in Nuclear Fusion Reaction, *JPS Conf. Proc.* **6**, 020056 (2015).
 - [43] Y. Nambu, Quasi-Particles and Gauge Invariance in the Theory of Superconductivity, *Phys. Rev.* **117**, 648 (1960).
 - [44] J. Goldstone, Field theories with «Superconductor» solutions, *Il Nuovo Cimento* **19**, 154 (1961).
 - [45] We thank Aurel Bulgac for pointing it to us.
 - [46] J.F. Liang, C.J. Gross, Z. Kohley, D. Shapira, R.L. Varner, J.M. Allmond, A.L. Caraley, K. Lagergren, and P. E. Mueller, Fusion probability for neutron-rich radioactive-Sn-induced reactions, *Phys. Rev. C* **85**, 031601, (2012).
 - [47] C.C. Sahm, H.G. Clerc, K.-H. Schmidt, W. Reisdorf, P. Armbruster, F.P. Hessberger, J.G. Keller, G. Münzenberg, D. Vermeulen, Fusion probability of symmetric heavy, nuclear systems determined from evaporation-residue cross sections, *Nucl. Phys.* **A441**, 316 (1985).

Supplemental online material for: "Novel Role of Superfluidity in Low-Energy Nuclear Reactions"

In the supplemental material we describe technical aspects related to: generation of the initial configurations, setting initial conditions for a collision and extracting kinetic energy of the fragments after collision. We provide also the evaluation of the contact energy of two superfluids within Ginzburg-Landau theory and the classical capture cross section taking into account nonzero phase differences between nuclear pairing fields. We show results of $^{240}\text{Pu}+^{240}\text{Pu}$ with $\Delta\varphi_p \neq \Delta\varphi_n$ quantifying contributions from neutrons and protons, and with ternary quasifission processes. Finally, we present typical results for asymmetric collisions of $^{86}\text{Zr}+^{126}\text{Sn}$ and non-central collisions of $^{90}\text{Zr}+^{90}\text{Zr}$.

TDSLDA CALCULATIONS FOR NUCLEAR REACTIONS

In this section we present the methodology which has been applied in order to:

- prepare initial configurations with two spatially separated nuclei,
- imprint the phase difference of the pairing fields of the two separated nuclei,
- collide them to simulate nuclear reactions within the framework of TDSLDA.

The initial states for the TDSLDA calculations were obtained as self-consistent solutions of the static SLDA equations which for both protons and neutrons have the following structure:

$$\begin{pmatrix} h - \mu & \Delta \\ \Delta^* & -(h^* - \mu) \end{pmatrix} \begin{pmatrix} u_k \\ v_k \end{pmatrix} = \varepsilon_k \begin{pmatrix} u_k \\ v_k \end{pmatrix}, \quad (2)$$

where h is the single-particle Hamiltonian and Δ is the pairing field, which are defined by functional derivatives of an energy density functional, and μ is the chemical potential (for either protons or neutrons). To reduce the number of diagonalizations needed to get the self-consistent solution, we have used the procedure similar to the one adopted to compute initial states for a vortex-nucleus system in the neutron star crust [1]. The lattice size is $20 \times 20 \times 64$ for head-on collisions and $20 \times 48 \times 64$ for non-central collisions. The lattice spacing is 1.25 fm and cut-off energy is set to $E_c = 100$ MeV.

One has to keep in mind that u -components and v -components, forming quasiparticle wave functions, behave differently when expressed in the coordinate representation. While the v -components are spatially localized around the two nuclei (as is always true for bound systems), the u -components are distributed over the whole

space. Thus one has to pay a particular attention when dealing with a system of two spatially separated nuclei, as they are entangled through the common u -components. For example, a discontinuity of the u -components is introduced if one generates separately ground states for two nuclei placed in smaller volumes and then combines them together in a larger volume. This is a typical method used in TDHF calculations, which is justified since the u and v components are decoupled for $\Delta = 0$ and one evolves only localized single-particle wave functions. In our case, however, this method will not work and therefore we generated self-consistent solutions for two nuclei in a box separated by a desired distance $\Delta x \approx 50$ fm. In order to avoid two nuclei to move apart because of the Coulomb repulsion, we have introduced an external potential:

$$V_{\text{ext}}(\mathbf{r}) = \sqrt{[V_0(x - x_0)]^2 + \delta^2}, \quad (3)$$

which is uniform in y - and z -direction. The parameter δ is a small constant which makes V_{ext} smooth around the center of the box ($x_0 = 40$ fm). Away from the center of the box the external potential is linear $V_{\text{ext}}(\mathbf{r}) \simeq V_0|x - x_0|$, and generates the constant force which compensates for the Coulomb repulsion. The parameter V_0 is adjusted to keep the two nuclei at rest during the self-consistent iterations. An example of the potential V_{ext} is shown in Fig. 5 (a). We used a shifted conjugate orthogonal conjugate gradient (COCG) method to compute densities during iterations [2]. Subsequently a direct diagonalization of the Hamiltonian (2) was performed, which provided the wave functions determining the initial configuration for both the projectile and the target nuclei contained in the common simulation box.

The generated initial states are characterized by the pairing field that has the uniform phase over the box. However, one can change the phase of one of the nuclei without affecting the energy of the system. This can be done dynamically, using the phase imprint technique commonly used in experiments on ultracold atomic gases. Namely, the additional external potential is applied for a certain time interval t_p . The external potential has the following form:

$$U(\mathbf{r}) = \begin{cases} U_0 s(x, 3.75, 2), & x \leq 3.75, \\ U_0, & 3.75 < x < 36.25, \\ U_0 s(x - 36.25, 3.75, 2), & 36.25 \leq x < 40, \\ 0, & x \geq 40, \end{cases} \quad (4)$$

where $s(x, w, \alpha)$ is a function which smoothly varies from 0 to 1 in an interval $[0, w]$:

$$s(x, w, \alpha) = \frac{1}{2} + \frac{1}{2} \tanh \left[\alpha \tan \left(\frac{\pi x}{w} - \frac{\pi}{2} \right) \right]. \quad (5)$$

An example of the potential is shown in Fig. 5 (b). Since the pairing field is proportional to the anomalous density $\nu = \sum_{0 < \varepsilon_n < \varepsilon_{\text{cut}}} u_n v_n^*$, the phase of the pairing field

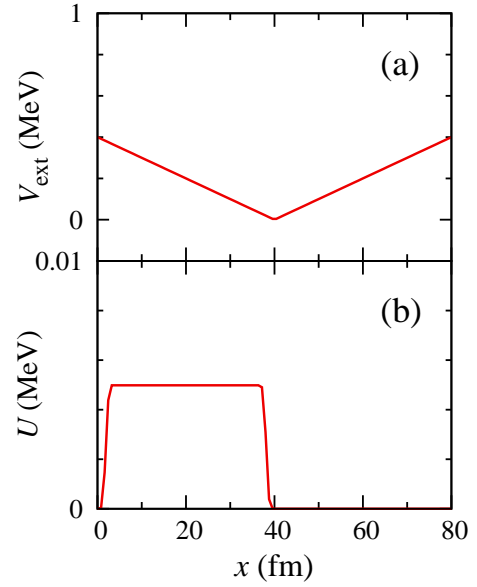


FIG. 5: (Color online) An example of external potentials used to keep nuclei at rest or for accelerating them (a) and for imprinting the required phase difference (b) as a function of x coordinate (along the collision axis). (a) V_{ext} defined by Eq. (3) is shown for $V_0 = 10^{-4}$ MeV and $\delta = 0.0003$ MeV. (b) U defined by Eq. (4) is shown for the case of imprinting the phase difference $\Delta\varphi = \pi$ during the time interval 1000 fm/c.

for the left half of the box ($x < 40$ fm) evolves in time as $\Delta(\mathbf{r}, t) = e^{2(\mu - U_0)t/\hbar} |\Delta(\mathbf{r}, t)|$, whereas for the right half ($x > 40$ fm) it evolves as $\Delta(\mathbf{r}, t) = e^{2\mu t/\hbar} |\Delta(\mathbf{r}, t)|$. Consequently after time t_p the phase for one side gets an extra shift $\Delta\varphi = 2U_0 t_p$. The height of the potential U_0 is adjusted to introduce the requested phase difference $\Delta\varphi$ within the time interval $t_p = 1000$ fm/c.

Finally, to collide two nuclei one needs to accelerate them up to a certain value of relative velocity. It is achieved by varying smoothly the slope parameter V_0 in Eq. (3) to a larger value $V_1 (> V_0)$ using the switching function. It is performed in a relatively short time of about 10 fm/c. Subsequently, the slope parameter V_1 is kept fixed until the two nuclei reach the desired relative velocity. Once this velocity is reached the external potential (3) is switched off (within the time of 10 fm/c), and the two nuclei collide. The collision energy is defined at the time when V_{ext} becomes zero.

ENERGY OF THE JUNCTION

Let us consider two superfluids being in contact and having the same superfluid density n_s , differing only by the phase of the order parameter $\varphi_{1,2}$ (see Fig. 6).

The energy of the junction is associated with the spatial variations of the phase on the length scale defined by the contact size. It can be easily evaluated within the

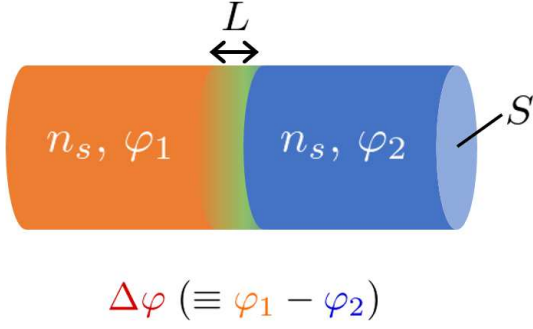


FIG. 6: (Color online) Schematic picture of a junction of two superfluids with different phases. This picture illustrates those quantities which enters Eq. (11): S is the area of the junction, L denotes the length scale over which the phase varies, n_s is the superfluid density, and φ_i ($i = 1, 2$) is the phase of the pairing field.

Ginzburg-Landau (G-L) approach. Namely, one can introduce the wave function of the condensate $\Psi(\mathbf{r})$ which is related to the superfluid order parameter with $|\Psi|^2$ being the density of particles that belong to the condensate. This quantity will be temperature dependent and clearly vanishes at critical temperature $T = T_c$. Superfluidity in fermionic systems is regarded as a condensate of Cooper pairs, thus $2|\Psi|^2$ has meaning of fermionic density. Consequently the wave function is expressed as

$$\Psi(\mathbf{r}) = \sqrt{\frac{n_s(\mathbf{r})}{2}} e^{i\varphi(\mathbf{r})}, \quad (6)$$

where $n_s \propto (1 - \frac{T}{T_c})$ is the superfluid density of fermions, and φ denotes the phase. In general the total density of particles separates into superfluid and normal components $n = n_s + n_n$ and in the zero temperature limit the latter vanishes. The total free energy of the system is given by

$$F_{\text{tot}} = \int (F_L(\mathbf{r}) + F_{\text{grad}}(\mathbf{r})) d\mathbf{r}, \quad (7)$$

where $F_L = \alpha(T)|\Psi(\mathbf{r})|^2 + \beta(T)|\Psi(\mathbf{r})|^4$ is the so-called Landau term. Since superfluid densities of both superfluids are equal this term does not contribute to the free energy of the junction. The gradient term has the form:

$$F_{\text{grad}} = \frac{\hbar^2}{2m^*} |\nabla\Psi(\mathbf{r})|^2, \quad (8)$$

where m^* is the effective mass of particles that form a condensate, and we assume $m^* = 2m_n$ which is the mass of the Cooper pair (m_n is the nucleon mass). Approximating the gradient by

$$\nabla\Psi(\mathbf{r}) \approx \sqrt{\frac{n_s}{2}} \frac{e^{i\varphi_2} - e^{i\varphi_1}}{L}, \quad (9)$$

where L is the length scale over which the phase varies from value φ_1 to φ_2 , one finds the free energy of the

junction (see also Fig. 6):

$$F_j = \frac{S}{L} \frac{\hbar^2}{2m_n} n_s \sin^2 \frac{\Delta\varphi}{2}, \quad (10)$$

where we have applied $|e^{i\varphi_2} - e^{i\varphi_1}|^2 = 4 \sin^2 \frac{\Delta\varphi}{2}$, denoting $\Delta\varphi = \varphi_1 - \varphi_2$ and SL is the volume of the junction. In the zero temperature limit the free energy becomes the energy of the junction and the superfluid density n_s becomes neutrons/protons density:

$$E_j = \frac{S}{L} \frac{\hbar^2}{2m_n} n_s \sin^2 \frac{\Delta\varphi}{2}. \quad (11)$$

KINETIC ENERGY OF THE FRAGMENTS

The total kinetic energy (TKE) of the outgoing fragments is evaluated as follows. We divide the simulation box into two regions by a plane parallel to the yz -plane, which defines left ($x < 40$ fm) and right ($x > 40$ fm) regions. Subsequently we compute the average mass and charge numbers and the center-of-mass of the fragments in respective regions, $A_{L,R}$, $Z_{L,R}$ and $\mathbf{R}_{L,R}(t)$. From the time derivative of the relative distance $\mathbf{R}(t) = \mathbf{R}_R(t) - \mathbf{R}_L(t)$, we compute the relative velocity $\mathbf{V}(t)$. We compute the TKE of the fragments when they are well separated spatially ($R \simeq 30$ fm) as follows:

$$\text{TKE} = \frac{1}{2} \mu(t) \mathbf{V}^2(t) + \frac{Z_L(t)Z_R(t)e^2}{|\mathbf{R}(t)|}, \quad (12)$$

where $\mu(t) = m_n A_L(t)A_R(t)/(A_L(t) + A_R(t))$ with m_n being the nucleon mass. To check the validity of this simple formula (12), we have also computed the TKE as follows:

$$\text{TKE} = \frac{\mathbf{P}_L^2}{2M_L(t)} + \frac{\mathbf{P}_R^2}{2M_R(t)} + V_{\text{Coul}}(t), \quad (13)$$

where $M_{L(R)}(t) = m_n A_{L(R)}(t)$, and the momentum is defined by

$$\mathbf{P}_{L(R)} = m_n \int_{L(R)} \mathbf{j}(\mathbf{r}, t) d\mathbf{r}. \quad (14)$$

The Coulomb energy can be evaluated from the proton density:

$$V_{\text{Coul}}(t) = e^2 \int_L \int_R \frac{\rho_p(\mathbf{r}_1, t) \rho_p(\mathbf{r}_2, t)}{|\mathbf{r}_1 - \mathbf{r}_2|} d\mathbf{r}_1 d\mathbf{r}_2. \quad (15)$$

We have found that the difference between Eqs. (12) and (13) is very small, at most a few MeV at certain times where fragments are close to each other and exhibit large deformations, which make multipole corrections relatively significant.

EFFECTS ON FUSION CROSS SECTION

The effect of the increased barrier can be included in the expression for the classical capture cross section. Namely, the classical expression reads:

$$\sigma(E) = \pi R^2 \left(1 - \frac{B}{E}\right) \quad (16)$$

where B defines the barrier height and $E > B$. The modification of this expression related to the pairing field phase difference reads:

$$\sigma(E) = R^2 \left(\Delta\varphi_{th}(E) - \frac{1}{E} \int_0^{\Delta\varphi_{th}(E)} B(\Delta\varphi) d(\Delta\varphi) \right), \quad (17)$$

where $R = r_0(A_1^{1/3} + A_2^{1/3})$ with $r_0 \approx 1.25$ fm, and $\Delta\varphi_{th}$ is the threshold angle below which the capture occurs at a given collision energy E . The expression requires $E \geq E_{\min}$, where E_{\min} is the lowest energy for capture without phase difference, *i.e.*, $\Delta\varphi_{th}(E_{\min}) = 0$. One can easily notice that for $E > E_{\max}$, where $\Delta\varphi_{th}(E_{\max}) = \pi$, the above formula is consistent with Eq. (16), with barrier height averaged over all angles: $\bar{B} = \frac{1}{\pi} \int_0^\pi B(\Delta\varphi) d(\Delta\varphi)$. Thus the effect of the phase difference on the capture cross section will enter through the effective barrier height averaged over all phase differences. In the energy interval $E_{\min} < E < E_{\max}$ one may use the above formula to extract the angle dependence on energy, directly from the excitation function. Namely in this case one obtains:

$$\frac{1}{R^2} \frac{d}{dE} (E\sigma(E)) = \Delta\varphi_{th}(E). \quad (18)$$

In practice, however, this quantity will be contaminated by other effects like, *e.g.*, quantum tunneling and nonzero width of barrier height distribution.

THE CASE OF $\Delta\varphi_p \neq \Delta\varphi_n$

In order to investigate the magnitude of contributions coming from proton and neutron superfluids separately, we have performed simulations of head-on collisions of $^{240}\text{Pu} + ^{240}\text{Pu}$ with different relative phases of proton and neutron pairing fields, *i.e.* $\Delta\varphi_p \neq \Delta\varphi_n$.

Let us first focus on the TKE of the fragments. In Fig. 7, we show the TKE as a function of the pairing phase difference for neutron superfluids, $\Delta\varphi_n$. The collision energy was set to $E \simeq 1.09V_{\text{Bass}}$, at which we have observed the most pronounced effect generating the largest TKE differences of about 25 MeV (see Fig. 3 (a) in the main text). The quantity V_{Bass} is the phenomenological fusion barrier [3].

In the figure one can see four curves representing $\text{TKE}(\Delta\varphi_n)$, although two of them practically coincide.

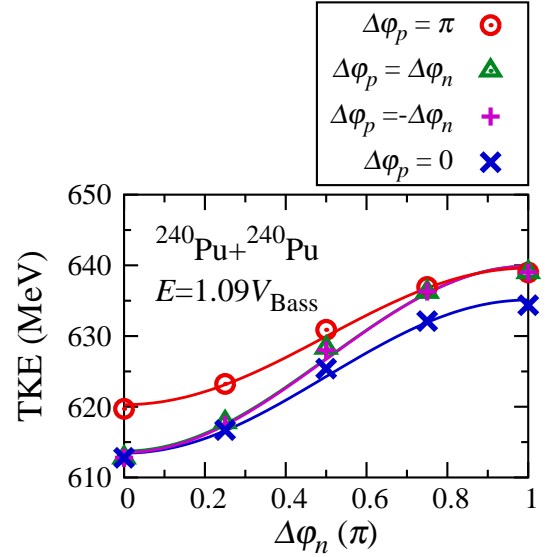


FIG. 7: (Color online) Total kinetic energy (TKE) of outgoing fragments in $^{240}\text{Pu} + ^{240}\text{Pu}$ collisions at $E \simeq 1.09V_{\text{Bass}}$ as a function of the pairing phase difference for neutron superfluids $\Delta\varphi_n$. The four different curves correspond to the following cases: green open triangles denote results obtained under condition that the imprinted phase difference for both neutron and proton superfluids is the same: $\Delta\varphi_p = \Delta\varphi_n = \Delta\varphi$ (This case has been shown in Fig. 3 (a) of the main text); pink plus symbols correspond to the case of proton superfluids having the opposite phase difference to that of neutron superfluids: $\Delta\varphi_p = -\Delta\varphi_n$; red open circles (blue crosses) correspond to the case of proton superfluids having the fixed phase difference at values: $\Delta\varphi_p = \pi$ (0). The solid curves represent fits to the data points with the expression $\alpha + \beta \sin \frac{\Delta\varphi_n}{2}$, taking α and β as parameters.

They correspond to the cases of $\Delta\varphi_p = \pm\Delta\varphi_n$ and indicate that the effect governing the TKE behavior is related to the solitonic excitation, as the energy of the junction is the same in both cases. This fact also confirms that the effects related to Josephson currents are indeed negligible, since in the case of $\Delta\varphi_p = \Delta\varphi_n$ protons and neutrons are transferred in the same direction, whereas in the case of $\Delta\varphi_p = -\Delta\varphi_n$ the directions of induced currents for protons and neutrons are opposite. The other two curves correspond to $\Delta\varphi_p = \pi$ and $\Delta\varphi_p = 0$ cases. The relative energy shift of these curves measures the magnitude of the contribution coming from the pairing phase difference for protons. Thus, clearly the total effect reflected in TKE comes from both proton and neutron superfluids, however the neutron contribution (≈ 21 MeV) is significantly larger than the proton contribution ($\approx 4-7$ MeV). This we attribute to the fact that neutrons play more important role in the neck formation, whereas contribution of protons is effectively suppressed by the Coulomb repulsion.

In Fig. 8, we show the average number of transferred neutrons (a) and protons (b) from the left nucleus to the

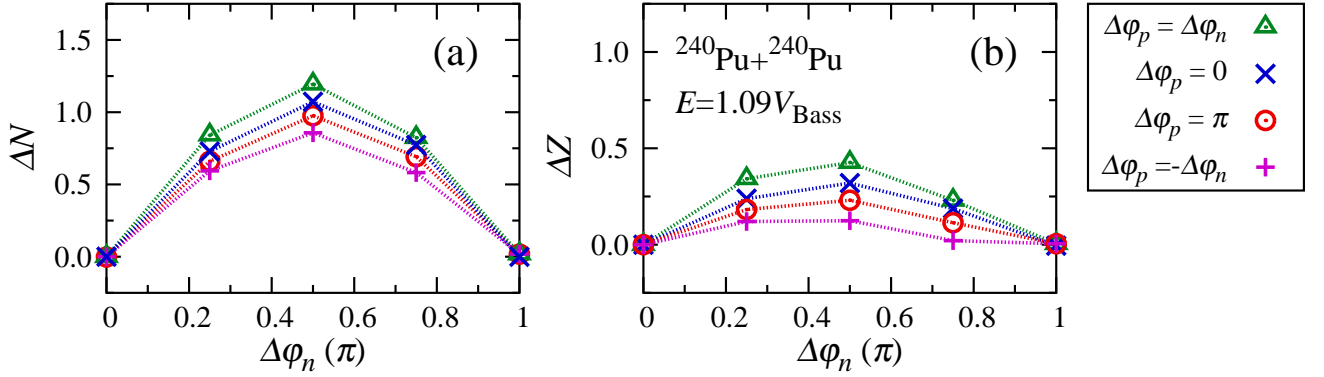


FIG. 8: (Color online) Average number of transferred neutrons (a) and protons (b) from the left to the right regions in $^{240}\text{Pu} + ^{240}\text{Pu}$ collisions at $E \simeq 1.09V_{\text{Bass}}$ for various types of phase differences. The horizontal axis is the pairing phase difference for neutron superfluids $\Delta\varphi_n$. Green open triangles show results where the phase is imprinted for both neutrons and protons the same amount ($\Delta\varphi_p = \Delta\varphi_n = \Delta\varphi$) (The same results as shown in Fig. 3 (b) of the main text). Pink plus symbols correspond to the cases where the phase difference for protons is opposite to that for neutrons ($\Delta\varphi_p = -\Delta\varphi_n$). Red open circles (blue crosses) correspond to the cases where the phase difference for protons is fixed to $\Delta\varphi_p = \pi$ (0).

right nucleus as a function of the pairing phase difference for neutrons, $\Delta\varphi_n$. All symbols are the same as in Fig. 7. In particular, green open triangles shown in Fig. 8 (a) denote the results shown also in Fig. 3 (b) of the main text. The amount of nucleons transferred during collisions is the largest for the case of $\Delta\varphi_p = \Delta\varphi_n$, *i.e.*, the case of both protons and neutrons flowing in the same direction. On the other hand, in the case of $\Delta\varphi_p = -\Delta\varphi_n$ the amount of transferred nucleons is the smallest, since induced Josephson currents for protons and neutrons have the opposite directions, and due to the mutual entrainment the magnitude of the currents is suppressed. Moreover, one can find a visible difference between the cases of $\Delta\varphi_p = 0$ and $\Delta\varphi_p = \pi$, despite the fact that the proton Josephson current is absent in both cases. It indicates that the solitonic structure in the proton pairing field plays also a role of a barrier suppressing neutron flow. Nevertheless in both cases ($\Delta\varphi_p = 0, \pi$) a small number of protons are transferred, and it is only due to the neutron Josephson current which entrain protons.

ASYMMETRIC REACTIONS

To examine the effects of the pairing phase difference on the dynamics in asymmetric reactions, we performed exploratory calculations for $^{86}\text{Zr} + ^{126}\text{Sn}$. In these reactions the phase difference is not well defined quantity, but it evolves in time and the evolution rate is determined by the difference of the nuclear chemical potentials. In the case of symmetric reactions (like $^{90}\text{Zr} + ^{90}\text{Zr}$) the collisions for the phase differences $\Delta\varphi$ and $2\pi - \Delta\varphi$, are connected by reflection symmetry (*i.e.* the symmetry transform one case into the other by exchanging the colliding nuclei) and therefore the relevant range for the

phase difference is limited to the interval $[0, \pi]$. This is no longer correct for asymmetric reactions and one has to consider all phase differences that span interval $\Delta\varphi \in [0, 2\pi]$. Nevertheless, we have observed qualitatively the same effect of the barrier enhancement due to the pairing as in $\text{Zr} + \text{Zr}$ reactions.

For the asymmetric reaction, at energy below the fusion threshold, the natural process that takes place is the particle transfer (due to difference in the chemical potentials). We observed that the phase difference can modify the amount of nucleon transfer. As an example in Fig. 9 we show the particle transfer for various phase differences of the initial state. Depending on the relative phase of the pairing fields 4–6 neutrons are transferred. It is due to the Josephson current that can either enhance or suppress the particle flow. The fluctuations in the particle transfer are about 2 particles, thus very similar to the other cases. The effects also induce indirectly variations for protons transfer.

TERNARY QUASIFISSION

In the case of $^{240}\text{Pu} + ^{240}\text{Pu}$ collisions at sufficiently high energies, we have observed exotic reaction dynamics. Namely, at energy $E \simeq 1.5V_{\text{Bass}}$ the composite system splits producing the third light fragment for all phase differences $\Delta\varphi$. Such a ternary quasifission process has been observed as well in TDHF approach [4], indicating the possibility of emission of a light fragment in the collision process. Interestingly, the third fragment is not at rest as it should be in the case of TDHF approach, where the left-right symmetry is being conserved in symmetric collisions in the center-of-mass frame. In our approach, however, the symmetry is broken due to the different phases of pairing fields of incoming nuclei. Conse-

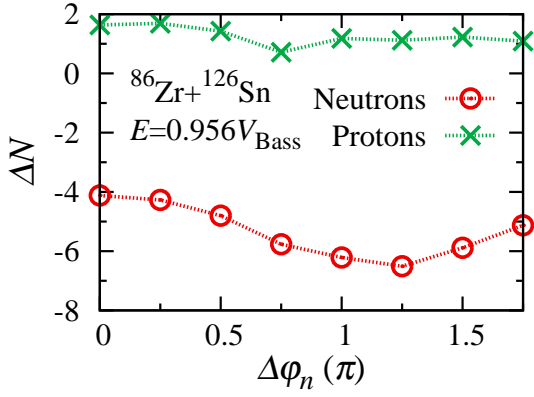


FIG. 9: (Color online) The neutron (red circles) and proton (green crosses) transfer for asymmetric reaction $^{86}\text{Zr}+^{126}\text{Sn}$ for the energy below the fusion threshold ($E = 0.956V_{\text{Bass}}$) as a function of phase differences for the neutron pairing field in the initial state.

quently, the Josephson current appears as a consequence of the symmetry breaking component in the pairing field. Therefore, it is not surprising that the third fragment is not at rest and is moving after splitting due to the current induced by the phase difference. Moreover, at the energies $E \simeq 1.3V_{\text{Bass}}$ and $E \simeq 1.4V_{\text{Bass}}$, we found that the number of fragments is affected by the phase difference. The situation is shown in Fig. 10. In this case, the solitonic structure prevents the formation of the third fragment from the neck region. The observed effects implicitly indicate the importance of the phase difference on the reaction dynamics even at relatively high energies, although one should keep in mind if TDSLDA description for such high energy collisions is valid.

NON-CENTRAL COLLISIONS

In order to investigate collision trajectories and their dependence on the pairing field phase differences, we have performed collisions with nonzero impact parameters. Since we solve TDSLDA equations in 3D Cartesian coordinates without any symmetry restrictions, we can also simulate non-central collisions. Namely, we have performed simulations for non-central collisions of $^{240}\text{Pu}+^{240}\text{Pu}$ and $^{90}\text{Zr}+^{90}\text{Zr}$. Similarly to central collisions, the phase difference prevents superfluid nucleons to enter the neck region. It causes the suppression of the neck formation and consequently the reduction of the contact time. In the non-central collisions, however, the small variations of the contact time have a dramatic effect on the collision trajectories. Consequently it affects both the scattering angle, as well as kinetic energy of the fragments and induces the correlation between these two quantities at a fixed impact parameter. In Fig. 11, we show an example of the non-central collisions

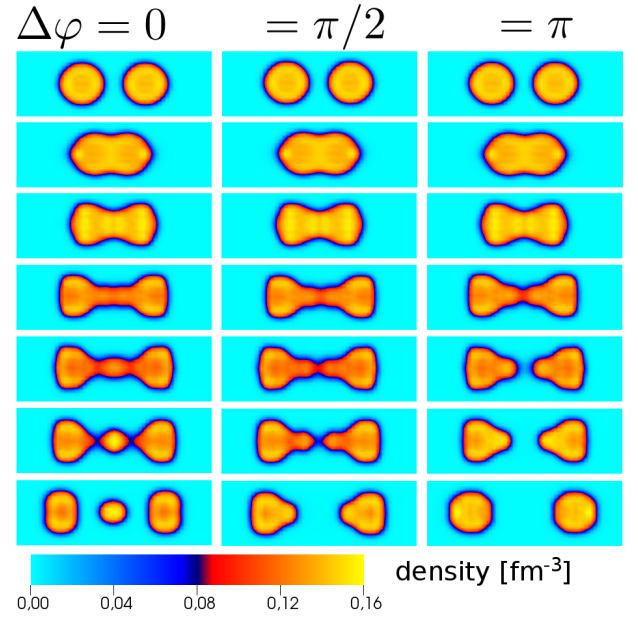


FIG. 10: (Color online) Snapshots of the density distribution on the reaction plane for $^{240}\text{Pu}+^{240}\text{Pu}$ collisions at $E \simeq 1.3V_{\text{Bass}}$, for three pairing phase differences: $\Delta\varphi = 0$ (left column), $\Delta\varphi = \pi/2$ (middle column) and $\Delta\varphi = \pi$ (right column). Contact time spans the interval 570–650 fm/c depending on the phase difference. The third fragment is created for the phase difference $\Delta\varphi \lesssim \frac{\pi}{4}$. For full movie, see [240Pu+240Pu.1.30V.mp4](https://youtu.be/7UstUB6DBn4) (<https://youtu.be/7UstUB6DBn4>).

of $^{90}\text{Zr}+^{90}\text{Zr}$, where the energy and the impact parameter are chosen in a such way that the system does not fuse, but splits after certain time. As is apparent from the figure, the pairing phase difference affects the contact time and consequently the scattering angles.

MOVIES

Central collisions of $^{240}\text{Pu} + ^{240}\text{Pu}$

The movies show sections along the reaction plane. Each movie displays 10 panels organized in grid 2 columns and 5 rows. The left column presents the total density (density of protons + density of neutrons), while the right column presents absolute value of the pairing field of neutrons. In each row dynamics of the system for pairing phase difference $\Delta\varphi$ is shown. The phase differences are from 0 (bottom row) to π (top row) with an increment $\pi/4$. The only difference in initial states is the phase difference, all other quantities (like energy, density distribution, etc.) are exactly the same (up to machine precision). Thus, all differences in the dynamics are due to the pairing effects. Below we provide 8 movies for different collision energies from a range $E \in [1.04 V_{\text{Bass}}, 1.50 V_{\text{Bass}}]$, where $V_{\text{Bass}} = 897.31 \text{ MeV}$ is

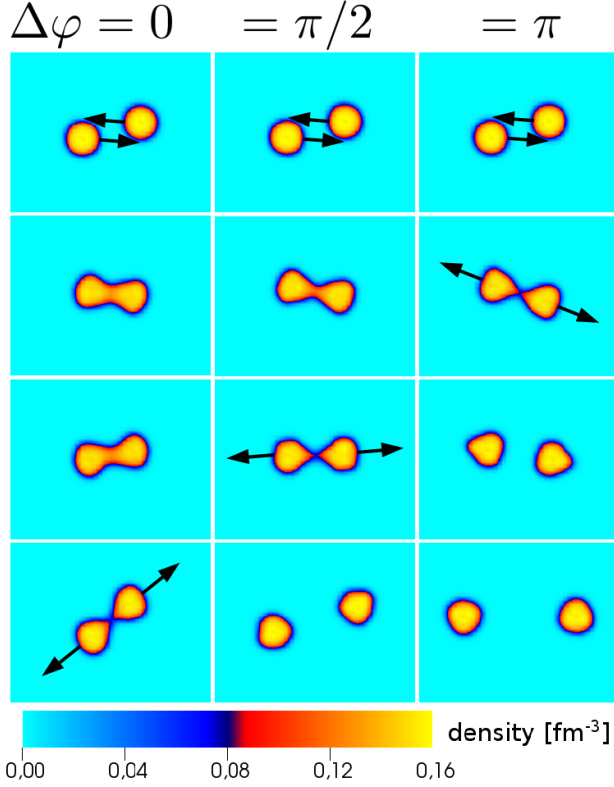


FIG. 11: (Color online) Snapshots of the density on the reaction plane for non-central collisions of $^{90}\text{Zr}+^{90}\text{Zr}$ at $E \simeq 1.4V_{\text{Bass}}$ ($b \approx 2$ fm), for three pairing phase differences: $\Delta\varphi = 0$ (left column), $\Delta\varphi = \pi/2$ (middle column) and $\Delta\varphi = \pi$ (right column). Contact time depends on the relative phase difference and it is approximately equal to: 1000, 840, and 720 fm/c, for phase differences 0, $\pi/2$, and π , respectively. For full movie, see 90Zr+90Zr_noncentral13.1.38V.mp4 (<https://youtu.be/UCCAN9ahNqA>).

the phenomenological fusion barrier [3]. The value of the collision energy is encoded in the file name.

1. File: 240Pu+240Pu_1.04V.mp4
YouTube: <https://youtu.be/foA33kCPT5g>
2. File: 240Pu+240Pu_1.07V.mp4
YouTube: <https://youtu.be/jiWpUUAe7Uw>
3. File: 240Pu+240Pu_1.09V.mp4
YouTube: <https://youtu.be/OYiBJ1PFVnA>
4. File: 240Pu+240Pu_1.15V.mp4
YouTube: <https://youtu.be/It1ZQRw9yDs>
5. File: 240Pu+240Pu_1.20V.mp4
YouTube: <https://youtu.be/bXTzRW2HgTQ>
6. File: 240Pu+240Pu_1.30V.mp4
YouTube: <https://youtu.be/7UstUB6DBn4>
7. File: 240Pu+240Pu_1.40V.mp4
YouTube: <https://youtu.be/rHLSWPYj798>

8. File: 240Pu+240Pu_1.50V.mp4
YouTube: <https://youtu.be/YH0wSPoU5ag>

Central collisions of $^{90}\text{Zr} + ^{90}\text{Zr}$

The movies are analogues to the movies for $^{240}\text{Pu} + ^{240}\text{Pu}$ collisions. For some energies not all panels are filled with data. These are situations that correspond to the fusion process. Moreover, for some cases one can notice that the system slowly rotates after collision. The effect originates from the fact that the collisions are not perfectly central (due to small numerical noise). Below we provide 12 movies for different collision energies from a range $E \in [0.98 V_{\text{Bass}}, 1.15 V_{\text{Bass}}]$, where $V_{\text{Bass}} = 192.47$ MeV and the value of the collision energy is encoded in the file name.

1. File: 90Zr+90Zr_0.98V.mp4
YouTube: <https://youtu.be/YcATJ6pMgD0>
2. File: 90Zr+90Zr_0.99V.mp4
YouTube: <https://youtu.be/amXMsxw1Wd0>
3. File: 90Zr+90Zr_1.00V.mp4
YouTube: <https://youtu.be/zE74gdLTgWw>
4. File: 90Zr+90Zr_1.02V.mp4
YouTube: <https://youtu.be/UEPiwEZDeYc>
5. File: 90Zr+90Zr_1.03V.mp4
YouTube: <https://youtu.be/Ubs3g12UW5U>
6. File: 90Zr+90Zr_1.04V.mp4
YouTube: <https://youtu.be/GysuioTC7mY>
7. File: 90Zr+90Zr_1.05V.mp4
YouTube: <https://youtu.be/cNbiadr7i48>
8. File: 90Zr+90Zr_1.11V.mp4
YouTube: <https://youtu.be/7Rc70bbnkx8>
9. File: 90Zr+90Zr_1.12V.mp4
YouTube: https://youtu.be/CZ_d19vIbtI
10. File: 90Zr+90Zr_1.13V.mp4
YouTube: <https://youtu.be/jv5iyFFrqBI>
11. File: 90Zr+90Zr_1.14V.mp4
YouTube: <https://youtu.be/sPH9PNEIVo4>
12. File: 90Zr+90Zr_1.15V.mp4
YouTube: https://youtu.be/U3t_xcdrWTA

Non-central collisions of $^{90}\text{Zr} + ^{90}\text{Zr}$

We also provide 3 movies demonstrating the impact of the phase difference on dynamics of non-central collisions. For better visibility we display only results for 3 phase differences: 0 (bottom row), $\frac{\pi}{2}$ (middle row) and π (top row). The collisions are for fixed collision energy and 3 different impact parameters.

1. File: 90Zr+90Zr_noncentral1_1.38V.mp4
YouTube: <https://youtu.be/bOLhIEmfFSQ>
2. File: 90Zr+90Zr_noncentral2_1.38V.mp4
YouTube: <https://youtu.be/N72VQJVo4aI>
3. File: 90Zr+90Zr_noncentral3_1.38V.mp4
YouTube: <https://youtu.be/UCCAN9ahNqA>

-
- * Electronic address: magiersk@if.pw.edu.pl, sekizawa@if.pw.edu.pl, gabrielw@if.pw.edu.pl
- [1] G. Wlazłowski, K. Sekizawa, P. Magierski, A. Bulgac, and M.M. Forbes, Vortex Pinning and Dynamics in the Neutron Star Crust, Phys. Rev. Lett. (in press).
 - [2] S. Jin, A. Bulgac, K. Roche, and G. Wlazłowski, Coordinate-Space Solver for Superfluid Many-Fermion Systems with Shifted Conjugate Orthogonal Conjugate Gradient Method, (2016), arXiv:1608.03711 [nucl-th].
 - [3] R. Bass, Fusion of heavy nuclei in a classical model, Nucl. Phys. **A231**, 45 (1974).
 - [4] C. Golabek and C. Simenel, Collision dynamics of two ^{238}U atomic nuclei, Phys. Rev. Lett. **103**, 042701 (2009).